Meeri Jännäri

# PARTIAL THYROCYTE-SPECIFIC $G\alpha_s$ DEFICIENCY LEADS TO RAPID-ONSET HYPOTHYROIDISM, HYPERPLASIA, AND PAPILLARY THYROID CARCINOMA-LIKE LESIONS IN MICE

Syventävien opintojen kirjallinen työ

Kevätlukukausi 2021

Meeri Jännäri

# PARTIAL THYROCYTE-SPECIFIC $G\alpha_s$ DEFICIENCY LEADS TO RAPID-ONSET HYPOTHYROIDISM, HYPERPLASIA, AND PAPILLARY THYROID CARCINOMA-LIKE LESIONS IN MICE

Integratiivisen fysiologian ja farmakologian laitos

Kevätlukukausi 2021

Vastuuhenkilö: Jukka Kero

TURUN YLIOPISTO
Lääketieteellinen tiedekunta

JÄNNÄRI, MEERI: Partial thyrocyte-specific $G\alpha_s$ deficiency leads to rapid-onset hypothyroidism, hyperplasia, and papillary thyroid carcinoma-like lesions in mice

Syventävien opintojen kirjallinen työ, 26 s.
Integratiivisen fysiologian ja farmakologian laitos
Maaliskuu 2021

---

Hypothyroidism is a condition where thyroid gland is not producing enough thyroid hormone, thyroxine, which regulates development, growth, and energy metabolism. The production of thyroxine is regulated by thyrotropin (TSH), a hormone secreted from the pituitary gland. TSH stimulates thyroid via thyrotropin receptor (TSHR). TSHR is a G-protein-coupled receptor and the stimulation of the receptor activates different intracellular signaling pathways. The main signaling pathway in thyrocytes is $G_s$-pathway, which stimulates the production of cyclic adenosine monophosphate (cAMP). G-proteins are composed out of α- and β-subunits. It is still not known how different G-proteins effect to thyroid pathophysiology. The aim of the study is to investigate if deletion of thyroid specific $G_s$-protein α-subunit ($G\alpha_s$) leads to hypothyroidism in a tamoxifen induced $G\alpha_s$ knock-out mouse model (iTGasKO).

Genotyping of the mice was performed from DNA isolated from skin tissue. Serum TSH and thyroxin levels were measured from blood samples. cAMP, qPCR, histological and immunohistochemical experiments were done from thyroid tissue samples collected from the mice. The mice were weighted and measured every two weeks. EchoMRI was used to measure body composition and runners were used to measure the activity of the mice. Statistical analyses were done using Prism7 software.

In general, iTGasKO mice were less active and in addition, weight loss and a lower amount of white adipose tissue were seen only in males. Unlike in human, in rodents it is typical to lose weight in hypothyroidism. In iTGasKO mice the serum thyroxine levels were lower and TSH levels higher compared to control mice ($P<0.01$) and cAMP production was decreased both in basal level and after stimulation ($P<0.01$). $G\alpha_s$ was expressed in small amounts in iTGasKO mice, but thyroid specific transcription factors and genes regulating thyroid hormone synthesis were downregulated. As an unexpected result, 6 months old iTGasKO mice were diagnosed to have papillary thyroid cancer-like lesions in histopathological studies. These areas were also shown to express $G\alpha_s$-protein. This leads to conclusion of high TSH levels and partial $G\alpha_s$ expression leading to cancer-like lesions. This mouse model is a new way to show how TSHR's $G_s$-pathway knock-out leads to hypothyroidism. However, different species carry different signaling pathways, so the changes may not be identical in human pathophysiology.

Key words: hypothyroidism, thyrotropin receptor, G-protein

# Partial thyrocyte-specific Gαs deficiency leads to rapid onset hypothyroidism, hyperplasia, and papillary thyroid carcinoma-like lesions in mice

Patyra K.1,2, Jaeschke H.1, Löf C.1,2, Jännäri M.1, Ruohonen S.T.1,2, Undeutsch H.1, Khalil M.3, Kero A.4, Poutanen M.1,2, Toppari J.1,4, Chen M.5, Weinstein L.S.5, Paschke R.6, Kero J.1,2,4

1Research Centre for Integrative Physiology and Pharmacology, Institute of Biomedicine, University of Turku, Kiinamyllynkatu 10, 20520 Turku, Finland; 2Turku Center for Disease Modeling, University of Turku, Kiinamyllynkatu 10, 20520 Turku, Finland; 3Department of Pathology & Laboratory Medicine, University of Calgary, 2500 University Dr. NW, Calgary, Canada; 4Department of Pediatrics, University Hospital, Kiinamyllynkatu 4-8, 20521 Turku, Finland; 5Metabolic Diseases Branch, National Institute of Diabetes and Digestive and Kidney Diseases (NIDDK), NIH, Bethesda, Maryland, USA; 6Arnie Charbonneau Cancer Research Institute, University of Calgary, 2500 University Dr. NW, Calgary, Canada.

Abbreviated Title: Tamoxifen-inducible thyrocyte-specific Gαs alpha-deficient mouse model

Key Terms: Thyroid, Gnas, Hypothyroidism, Papillary thyroid cancer, Thyroglobulin, Cre mouse line, Gs alpha flox

Word count:

Number of figures: 6 figures, and 2 supplementary figures and 2 supplementary tables

Correspondence to: Jukka Kero

Research Centre for Integrative Physiology and Pharmacology

Institute of Biomedicine

University of Turku, Kiinamyllynkatu 10

20520 Turku, Finland

Phone: +358 2 3337576

Email: jukka.kero@utu.fi

Supporting grants: Finnish Pediatric and Medical Foundations, EVO grant from Turku University Hospital, Academy of Finland, Sigrid Juselius Foundation, Jalmari and Rauha Ahokas Foundation (JK), Turku University Foundation and Lifespan travel grant (KP).

ABSTRACT

The thyroid function is controlled by the thyroid-stimulating hormone (TSH), which binds to its G protein-coupled receptor (TSHR) on thyrocytes. TSHR can couple to all G protein families, but it mainly activates the Gs- and Gq/11-mediated signaling cascades. To date, there is still a knowledge gap concerning the role of the individual G protein cascades in thyroid pathophysiology and their putative clinical significance. Here, we demonstrate that the thyrocyte-specific deletion of Gαs in adult mice (iTGαsKO) rapidly impairs thyrocyte function and leads to hypothyroidism. Consequently, the iTGαsKO mice show reduced food intake, activity and altered brown adipose tissue histology. However, the body weight and the amount of white adipose tissue were decreased only in the iTGαsKO males. Unexpectedly, hyperplastic follicles and papillary thyroid cancer-like lesions with increased proliferation and slightly increased pERK1/2 staining were found in iTGαsKO mice at an older age. These tumors developed from nonrecombined thyrocytes still expressing Gαs in the presence of highly elevated serum TSH. In summary, we report that partial thyrocyte–specific Gαs deletion leads to hypothyroidism, but also to tumor development in thyrocytes with remaining Gαs expression. Thus, these mice are a novel model to elucidate the pathophysiological consequences of hypothyroidism and the TSHR/Gs/cAMP – mediated tumorigenesis.

## INTRODUCTION

The thyroid gland produces and secretes thyroid hormones (TH), which play a fundamental role in vertebrate development, energy metabolism, thermogenesis and growth (1). The main regulator of the TH synthesis, growth and differentiation is the thyroid-stimulating hormone (TSH), which is secreted by the anterior pituitary. TSH binds to its G protein-coupled receptor (TSHR) expressed on the basolateral membrane of thyrocytes, and mainly activates the Gs/adenylate cyclase signaling. Activation of the Gs-pathway then leads to an increased production of intracellular cyclic adenosine monophosphate (cAMP) and the activation of various cellular functions in thyrocytes. However, TSHR can potentially couple to all four G protein families at least in vitro (2). Up to date, the physiological significance has primarily been demonstrated for the Gs- and Gq/11-mediated signaling pathways. However, but the detailed role of the different TSHR/G protein-coupling in thyroid pathophysiology is not known. In our previous study, we reported the importance of Gαq/11 for iodine organification, TH release and goiter growth in vivo (3). In patients with congenital hypothyroidism and nonclassical resistance to TSH, a TSHR mutation with a Gq/11-dominant coupling defect has been suggested to cause different phenotypes compared to TSHR mutations with impaired the Gs signaling (4,5). While the key role of Gs in TH synthesis, secretion, iodine uptake, and thyrocyte proliferation has been extensively investigated in vitro (6,7), an in vivo model has not been characterized so far.

Gαs is a ubiquitously expressed G protein encoded by Gnas. Inactivation of the Gαs in an animal model (8) or loss of function mutations in humans leads to complex phenotypic manifestations, which are dependent on the genomic imprinting (9). The

role of Gαs in thyroid tumor growth has been investigated in different cancer models, showing that the inactivation of Gs or TSHR signaling strongly attenuates tumor development (10,11). Furthermore, activating mutations in the Gαs or a constitutive activation of Gs-signaling pathway have been associated with hyperthyroidism and thyroid adenomas in mice (12,13). Analogously, activating mutations in Gαs or in the TSHR lead to constitutive receptor activation and cAMP production, which present well-known etiologies of hyperfunctioning thyroid adenomas (14–17). However, it remains unclear, whether the constitutive activation of Gs- or TSHR-mediated signaling alone triggers the expansion of the adenoma and development of thyroid cancer. Alternatively, it may simply promote the tumor growth after genetic alterations in oncogenes (18) or other genes (19). A clinical association between elevated serum TSH levels and a higher risk of thyroid malignancies has been reported (20). Moreover, the treatment with supraphysiological doses of thyroxine is recommended to suppress serum TSH, and to reduce the risk of a recurrent malignancy in patients with high risk thyroid cancer (21).

Inactivating TSHR mutations (22) or the complete absence of TSHR (23) lead to hypothyroidism. Depending on the age of initiation and the duration of hypothyroidism, it may have a deleterious impact on the development and growth. In addition, to these genetic models presenting with severe congenital forms of hypothyroidism, pharmacologically induced hypothyroidism models have been commonly studied (24). However, the latter model used anti-thyroid drugs (methimazole or propylthiouracil), which inhibit the TH synthesis with possible side effects. To study the development of hypothyroidism and Gαs-mediated signaling in the thyroid, we generated thyrocyte-specific tamoxifen-inducible Gαs deficient (iTGαsKO) mice. Here, we demonstrate that the genetic ablation of Gαs leads to rapid onset hypothyroidism and consequent sex-dependent metabolic alterations, but also unexpectedly, to the development of papillary thyroid carcinoma-like (PTC-like) lesions in areas with remaining Gαs expression.

## RESULTS

### Generation of thyrocyte-specific tamoxifen-inducible Gαs -deficient mice

Inducible thyrocyte-specific Gαs-deficient mice (iTGαsKO) were generated by crossing the mouse line expressing the tamoxifen-inducible Cre-recombinase under the control of the thyroglobulin promoter (25) with mice carrying loxP sites flanking exon 1 of the Gnas gene (26) (Fig. 1A). Cre-mediated thyrocyte-specific recombination was confirmed by PCR with genomic DNA, which showed the presence of the recombined allele after tamoxifen treatment. A weak PCR product of the recombined allele was also detected in non-treated Cre-positive Gnas floxed animals, indicating a low Cre-mediated recombination activity in the absence of tamoxifen (Fig. 1B). The thyrocyte-specific Gαs deficiency was also confirmed in primary cells, in which thyrocytes from iTGαsKO mice showed a significantly lower basal cAMP production and an approximately five times lower cAMP response to high dose (10 mIU) TSH stimulation compared to tamoxifen treated controls (Fig. 1C). Furthermore, strong Gαs staining was detected in the thyrocytes, of control mice, but only a weak staining was observed in the

thyroids of iTGαsKO mice (Fig. 1D). Taken together, these results indicate that Gs signaling is strongly reduced, but not completely absent in the thyroids of iTGαsKO mice.

The thyrocyte-specific deletion of the Gαs leads to a rapid onset of hypothyroidism

The tamoxifen-induced recombination was induced at 4 weeks of age. The thyroid function tests (TFT), thyroid and pituitary weights were then assessed at two and six months of age. Severe hypothyroidism developed already one month after the induction, as demonstrated by highly elevated serum TSH and strongly decreased total T4 levels in both female and male iTGαsKO compared to control mice (Fig. 2A, B). Despite the detection of the recombined allele by PCR in the vehicle treated controls (Cre+/-, Gαsfl/fl), no significant difference in TSH or total T4 concentrations was observed between the control groups (Supplementary fig. 1A-D). This indicates that a small rate of Cre-mediated recombination without tamoxifen-induction did not physiologically affect TFTs in this model. In hypothyroid iTGαsKO mice, serum TSH levels were up to 150-times higher at two and six months of age than in controls (Fig. 2A, B). In addition to hypothyroidism, thyroid weights in both genders of the 2- and 6- month old iTGαsKO mice were significantly decreased compared to controls (Fig. 2C). Furthermore, in line with the highly elevated serum TSH levels in iTGαsKO mice, the pituitaries of both males and females were significantly larger than in the control animals (Fig. 2D).

The consequences of hypothyroidism were monitored by following the body weight and growth after tamoxifen induction. The body weights of the iTGαsKO males were significantly reduced at the age of 8 weeks compared to their control littermates (Fig. 3A). Later the iTGαsKO males were approximately 15% leaner than the controls after six months. Interestingly, there was no significant difference in body weight in female iTGαsKO mice versus controls despite the similarly elevated serum TSH and decreased total T4 levels, reduced food consumption and body temperature (Fig. 3B) in the male and female iTGαsKO. This was accompanied with a reduced amount of total adipose tissue mass, estimated with the EchoMRI quantification (Fig. 3C, left), and smaller white adipose tissue fat pads (Fig. 3C, right). Nevertheless, the overall histology of the white adipose tissue was not altered (Supplementary fig. 2A). The adipocytes of the brown adipose tissue in iTGαsKO mice contained predominantly smaller lipid droplets compared to controls (Supplementary fig. 2B). Furthermore, the running wheel activity during the dark cycle was generally lower in both male and female iTGαsKO than in controls (Fig. 3D). There was no significant change in the growth velocity monitored by repeated tail length measurements (Supplementary fig. 1E, F).

Thyroid histology, morphometric analysis, and gene expression

As expected, most of the thyrocytes in iTGαsKO mice showed a weak Gαs staining one month after the induction of the Gαs deletion. The thyroid histology showed thinner thyrocytes and reduced follicle area in the iTGαsKO mice compared to controls (Fig. 1 and 4A-F). At 2 months of age, the thyrocyte proliferation rate, indicated by the Ki67 positive cells, was low and comparable between iTGαsKO and controls (Supplementary fig. 2C). Furthermore, the expression of thyrocyte-specific transcription factors and

genes regulating TH synthesis were downregulated in both male and female KO compared to controls. In general, the downregulation was stronger in thyroids from iTGαsKO males (Fig. 4G), in which specifically the expressions of Hhex, Pax8, Tg, Tpo, Nis and Dio1 were significantly reduced. Similar, but less pronounced downregulation of Hhex, Nkx2.1, Tg, Dio1 gene expression was measured in iTGαsKO females (Fig. 4H). No changes in thyroidal gene expression of the genes related with oxidative stress were observed between iTGαsKO and controls (Fig. 4G, H). In line with the reduced gene expression of Nkx2.1, immunohistochemical staining with anti-Nkx2.1 antibody presented weaker staining in iTGαsKO mice thyroids versus controls (Supplementary fig. 2D).

## The partial thyroid-specific Gαs deletion leads to the development of hyperplastic follicles and PTC-like lesions in areas with residual Gαs immunostaining

The long-term impact of the Gαs deletion on thyroid histology was evaluated at six months of age. Interestingly, although the thyroid weights in iTGαsKO were not increased and a large part of the thyrocytes remained thin, several hyperplastic and neoplastic lesions were observed in all 6-month-old iTGαsKO thyroids of both sexes. The detailed analysis of these neoplastic lesions presented several typical features of papillary thyroid carcinomas, such as overlapping nuclei, nuclei with grooves, and nuclear enlargement (Fig. 5). Overall these neoplastic lesions covered up to 6% of the thyroid sections analyzed (with a range 1-6% of the total section area, n = 5 iTGαsKO mice, 4 sections/thyroid) (Fig. 5). Furthermore, strong Gαs staining in these altered areas was observed using the anti-Gαs antibody, indicating an incomplete deletion of the Gαs-protein in these thyrocytes (Fig. 6A). Moreover, the neoplastic areas were positive for Nkx2.1 and also strongly stained with the proliferation marker Ki67 (Fig. 6B, C). The TSH-mediated activation of extracellular signal-regulated protein kinases 1 and 2 (ERK1/2) was studied by immunohistochemistry using total-ERK1/2 (tERK1/2) and phospho-ERK1/2 (pERK1/2) antibodies. No changes in tERK1/2 staining were observed between Ctrl and KO thyroids (Fig. 6D). Interestingly, slightly increased pERK1/2 staining was detected in the hyperplastic and neoplastic areas of the iTGαsKO, whereas only a few thyrocytes were stained positive for pERK1/2 in the control thyroids (Fig. 6D, E).

To test if the PTC-like lesions found in iTGαsKO thyroids harbored any known common genetic mutations corresponding to the human hotspot area in BRAF (c.1799 c>t, V600E), genomic DNA from the microdissected neoplastic areas was isolated and sequenced. However, no mutations were found in seven microdissected tumor lesions from iTGαsKO mice.

## DISCUSSION

The TSH mediated Gs/cAMP/PKA signaling is the main regulator of thyrocyte growth and differentiation. The constitutive activation of this signaling pathway can lead to the development of autonomously functioning adenomas (17,27). Furthermore, increased levels of TSH together with the genetic alterations in known oncogenes (28) or other genes (19) can promote tumor growth. However, it has been unclear, whether the constitutive activation of GNAS or TSHR mediated signaling alone can trigger the expansion of the adenoma and the development of thyroid cancer. Here, we demonstrate that a partial inactivation of Gαs/cAMP-mediated signaling in thyroids of adult mice impairs TH production and causes rapid onset hypothyroidism. However, in parallel, chronically highly elevated TSH together with the remaining of Gαs in a small percentage of the thyrocytes lead to the development of PTC-like lesions in these mice. This was an unexpected finding, as a spontaneous development of PTCs in hot thyroid nodules without alterations in oncogenes has been only very rarely observed (11,29–32). Also, in rodents, the prolonged administration of anti-thyroid drugs and simultaneous TSH stimulation is primarily associated with the development of benign tumors and very rarely with thyroid cancer (33).

Our data support previous epidemiological studies, which suggest an association between elevated TSH levels and an increased risk of developing thyroid cancer (34,35). In our model, the Gαs protein and the overall TSH-stimulated cAMP response is strongly reduced one month after the genetic deletion of the Gnas exon 1 in adult mice, leading to the downregulation of several TSH responsive genes and highly elevated serum TSH levels. At this early time-point, no altered areas in thyroid were observed. However, thyroid hyperplasia and PTC-like lesions were detected in six-month-old iTGαsKO mice. The presence of strong Gαs staining in all hyperplastic and PTC-like areas suggests that the tumors originate from the non-recombined thyrocytes expressing the intact Gαs. Based on this data, Gαs is required for tumor development. However, also the Gα q/11 and other TSH mediated signaling pathways are activated due to very high serum TSH levels, which could contribute to promoting tumorigenesis. In contrast to iTGαsKO mice, mice lacking Gαq/11 in the thyrocytes show no tumors or goiter development despite highly elevated TSH levels and intact cAMP signaling (3). This suggest that the simultaneous activation of both Gαq/11 and Gαs pathways are required for the PTC-like phenotype. Similarly, in the thyroid-specific Braf (V600E) mouse model, which develop aggressive PTCs, the Gαs deletion attenuated, but did not prevent the development of PTC, suggesting that multiple pathways are involved (36). The increased pERK1/2 staining in the hyperplastic and PTC-like areas in iTGαsKO thyroids indicate that the activation of MAPK signaling pathway in these lesions requires Gαs. This is in line with in vitro studies describing that TSH and/or cAMP can augment the growth-factor stimulated pERK1/2 phosphorylation (7,37). However, the highly elevated TSH concentration alone in a mouse goiter model does not lead to an increased phosphorylation of ERK1/2 or CREB (38). Thus, additional events are needed for PTCs to occur. The requirement of TSHR signaling in BRAFV600E induced PTC (36) or other thyroid cancer mouse models (11,39) has been reported in several studies. Furthermore, it has been demonstrated that TSH may trigger advanced clinical stage of tumor, extrathyroidal extension, lymph node metastasis, genomic instability, or endure the oncogene induced senescence in the aforementioned mouse models (39,40).

Nevertheless, the precise role of TSH in the etiology of PTC still remains unraveled. In humans, autonomously functioning thyroid adenomas are almost always benign (30,31). Moreover, there is no evidence of a gradual adenoma–carcinoma transition leading to PTC. In PTC, especially the activation of the MAPK signaling pathway has been linked to malignant thyroid growth. Moreover, mutations in oncogenes like BRAF (V600E) are frequently found in PTC (18). However, in our iTGαsKO model, no mutations in Braf hotspot area in the thyroid tumors were found suggesting other mechanisms play a role in the activation of this pathway.

Despite the presence of Gαs, highly elevated TSH levels and hyperplastic and tumorous lesions in the thyroid of iTGαsKO mice, hypothyroidism persisted at least five months after the induction of the genetic Gαs deletion. This indicates that this relatively small part of the hyperplastic or PTC areas is insufficient to compensate the deficient TH synthesis. However, a longer follow-up is necessary to reveal whether the growth of these lesions would lead to increased serum TH concentration.

In our study, the thyrocyte-specific inactivation of Gαs in adult mice lead to severe acute hypothyroidism. To the best of our knowledge, this represents the first inducible hypothyroidism mouse model in which hypothyroidism is induced in adult mice via thyroid-specific gene deletion. Therefore, our mouse line might differ from the previous congenital or pharmacologically induced hypothyroidism models (23). In both sexes of the Gαs deficient mice, the serum TSH levels were highly elevated and T4 levels were below the normal range already at one month after tamoxifen induction. This confirms that the Gs-mediated TH synthesis cannot be compensated by other TSH-activated signaling pathways despite the highly elevated serum TSH levels in the iTGαsKO mice compared to control mice. This clearly differs from the thyroid-specific Gαq/11-deficient mice, which develop subclinical hypothyroidism a few months after the Gαq/11-deletion (3). Furthermore, a clear physiological sex-difference was observed in our hypothyroid model. The hypothyroid iTGαsKO males showed less weight gain associated with reduced total body fat, food intake, body temperature, and activity. In contrast, no weight difference was seen in hypothyroid iTGαsKO females compared to controls, despite of the similar degree of hypothyroidism, reduced food intake, body temperature and activity. Unlike in humans, where weight gain is a classical symptom of hypothyroidism, the weight loss has been reported when hypothyroidism is induced pharmacologically in rodents (41). The reason for the different adaptation of body weight in hypothyroidism between male and female iTGαsKO mice remains unclear, but it may reflect e.g. sex-specific differences in tissue deiodinase activities as suggested previously (42). Additionally, TH stimulate growth hormone secretion in rodents, which could partly explain the impaired growth and weight gain in hypothyroid rodent models (43).

In conclusion, we demonstrate the essential role of Gαs in TH synthesis in vivo. Furthermore, we report that chronically elevated TSH can lead to the development of PTC-like lesions in the absence of known oncogenic alterations in mice. This model is a powerful tool to study adaptation mechanisms in hypothyroidism and detailed signaling pathways in TSH/Gs-mediated tumor development.

## MATERIALS AND METHODS

### Mouse model generation, husbandry and genotyping

Thyrocyte-specific Gαs-deficient mice were generated by crossing the mouse line expressing the tamoxifen-inducible Cre recombinase under the control of the thyroglobulin promoter (25) with mice carrying a floxed allele of Gnas exon 1 (26) (Fig. 1A). The control mice were tamoxifen (Tam) treated Cre-/-, Gαsfl/fl mice unless otherwise stated. The tamoxifen–inducible Cre mice had C57Bl/6N background, and the Gαs floxed mice had a mixed genetic background (26). The analysis was done for F3-F4 generation. The animals were housed at the Central Animal Laboratory, University of Turku, under controlled conditions (12h light, 12h dark, 21±1°C) and ad libitum access to water and pelleted chow RM3 (E) Soya Free, Special Diet Services, Essex, UK) containing 1.6 µg/kg of iodine.

Tamoxifen (Sigma Aldrich, MO, USA) was dissolved in 99.6% pure ethanol in a concentration of 100 mg/ml, aliquoted and stored in -20oC. Before injection, tamoxifen solution was thawed, gently heated and diluted in commercially available rapeseed oil (1:10). The KO (Cre+/- Tam) and the tamoxifen control (Cre-/- Tam) group of mice at the age of 4 weeks were injected ip with 1 mg (100 ul) of freshly prepared tamoxifen solution (5 mg/mouse). Cre controls (Cre+/- Veh) and vehicle controls (Cre-/- Veh) at the age of 4 weeks were injected with 100 ul of 99, 6% ethanol diluted 1:10 with rapeseed oil.

### Serum TSH and thyroid hormone measurements

After tamoxifen injection, total T4 was measured every 4 weeks from mice from all groups (n=5 per group) for 5 months using total T4 kit ELISA kit (NovaTec, Germany) according to the manufacture's protocol. Absorbance was measured at 450 nm with Wallac 1420 Victor2 plate reader (Perkin Elmer, MA, USA) and total T4 concentration was calculated with MultiCalc 200 software. Serum TSH was measured with Mouse Pituitary Magnetic Bead Panel (Merck Millipore, Germany). Fluorescent intensity was measured with the Luminex 200 (Austin, TX, USA) and data were calculated with the Luminex Xponent software v. 3.1.

### Primary cell culture and cAMP measurements

After two months of tamoxifen injection (3 months of age), thyroid follicles were isolated and thyrocytes grown as described previously Jeker et al. (44), with minor modifications. Briefly, thyroids were dissected and placed into sterile DMEM media (Sigma-Aldrich, MO, USA) with 10% FCS (Biowest, Nuaillé, France) and cut into smaller pieces with a scalpel and subsequently digested with 225 U/ml Collagenase and 75 U/ml Hyaluronidase (Stemcell Technologies, Canada) and 3 U/ml Dispase (BD biosciences, San Jose, CA) for 30 min at 37□C on a sample mixer. After digestion, the samples were centrifuged at 1500 rpm for 5 min, then washed with PBS. The follicles were resuspended in DMEM media containing 10% FCS and complemented with 10 µg/ml of insulin, 5 µg/ml of transferrin, 3.5 ng/ml of hydrocortisone, 10 ng/ml somatostatin and 2 ng/ml Gly-His-Lys acetate (Sigma-Aldrich, MO, USA) on a 96-well

plate. After 3-4 days in cell culture, the cells were washed three times with PBS and 200 µl of fresh cell culture media without serum and hormones was added, containing 1 mM 3-Isobutyl-1-methylxanthine (IBMX) (Sigma-Aldrich, MO, USA). The cells were stimulated with 1 and 10 mU/ml of bTSH (Sigma-Aldrich, MO, USA) for 1h and the media containing extracellular cAMP were collected from the wells. Intracellular cAMP was extracted by incubating the cells for 30 min with 0.1 M HCl on ice. Extra- and intracellular cAMP, was measured with radioimmunoassay (RIA) as previously described (45).

## Quantitative Real-Time PCR (qRT-PCR)

Samples were snap frozen in liquid nitrogen and stored at -88 oC. Samples were homogenized by using stainless metal beads (QIAGEN, Germany) at 50 rpm for 2 min. Total RNA was isolated with TRIsure™ reagent (Bioline, UK) according to the manufacture's protocol. RNA concentration and purity was measured with NanoDrop™ ND-1000 (Thermo Scientific, MA, USA) UV-VIS spectrophotometer at 260/280 and 260/230 nm. Furthermore, RNA integrity was evaluated in 1% agarose gel and visualized with Midori Green Direct reagent (Nippon Genetics, Japan). RNA (500 µg) was treated with DNase I amplification grade (Sigma Aldrich, MO, USA) and transcribed to cDNA by using SensiFAST™ cDNA Synthesis Kit (Bioline, UK) according to the manufacture's manual. Then cDNA was diluted 1:100 in Braun sterile water (Braun, Germany) and qRT-PCR was performed in 10 µl reaction volume using SYBR Green PCR Master Mix (Applied Biosystems, CA, USA) accordingly to manufacture's protocol. Samples were normalized to the geometric mean of the Cyclophilin A (Ppia) and the Ribosomal protein L19 (Rpl19) expression. Efficiency of primer binding was established by using a standard curve made from pooled control samples in the following dilutions: 1:10, 1:100, 1:1 000 and 1:10 000. The final concentration of primers was 500 nM. Relative gene expression was calculated with the Pfaffl method. Relative gene expression from each group (n=5) was compared to the Cre-/- Tam control group (n=5). The list of used primers with temperatures of annealing is attached in the Table 1.

## Histology, immunohistochemistry and morphometric analysis

Histology samples were fixed in 10% neutral buffered formaline (Oy FF-Chemicals Ab, Finland), dehydratated in 50 % EtOH for 1 h in RT, 70 % o/n in +4 oC and embedded in paraffin. Samples were cut with a microtome (Leica, Germany) into 4 □m sections. Immuonohistochemistry and Hematoxylin-Eosin (HE) stainings were performed as described previously (46). The thickness of the thyrocytes and the follicle area were calculated with Panoramic Viewer software v. 1.15.4 (3DHistech Ltd., Hungary. The list of used antibodies is attached in the Table 2.

## Papillary thyroid cancer-like (PTC-like) classification and genotyping

Formalin-fixed paraffin-embedded mouse thyroids were cut by using a microtome (Leica, Germany) into 4 µm section on membrane slides 1.0 PEN (Carl Zeiss,

Germany). Slides were deparaffinized with xylene and stained for 30 second with Mayer's hematoxylin with standard procedure. Pictures at 50x magnification of whole thyroids were taken by using Leica DMRBE microscope (Leica, Germany). The lesion was classified as PTC-like when one or more of the following PTC features were observed: overlapping nuclei, nuclei with grooves, or pseudoinclusions. Selected PTC-like lesions were cut with a PALM MicroBeam (Carl Zeiss, Germany) laser capture microscope. DNA was extracted by using an in-house isolation method (protocol on request). PCR was performed for mouse Braf (codon 600). PCR products were separated in 1.5 % standard agarose gel for 30 minutes at 120 V in 1xTBS. PCR products were cutted from the gel and purified with the NucleoSpin Gel and PCR Clean-up kit (Macherey-Nagel, Germany) according to manufacturer's protocol. Purified products were sequenced (GATC Biotech AG, Germany) and analyzed for plausible hot-spot mutations with FinchTV 1.4.0 software (PerkinElmer, Finland). The sequence for the BRAF (c.1799 c>t, V600E) genotyping primers were as follow: F: 5'-TTCATGAAGACCTCACGGTAAAA-3' and R: 5'-GTGAGTAGTGGGAACTGTGAAAG - 3'.

## Growth, bodyweight, temperature and body composition

Body weight and tail length of mice from each group (n≥5) were followed-up for 5 months every two weeks after tamoxifen induction. Body composition of the mice at the age of 6 months were measured with a body composition analyzer based on quantitative nuclear magnetic resonance (Echo MRI-700, EchoMRI Houston, TX, USA). Lean mass, fat mass and total water was adjusted to the weight of mice and percentage value was calculated.

For measuring food consumption, mice (n = 9/group) at the age of 7 weeks were divided one week before into groups of 2-3 animals per cage. The provided food was weighed before and after four days. Body temperature was measured with a rectal probe (Physitemp instruments Inc,, NJ, USA). At the age of 8 weeks, mice (n= 6-9 per group) were single caged, and after 48 hours of adaptation, measurement of activity was carried-out for the next 72h using wireless running wheels ENV-047 (MedAssociates Inc, USA). Counts from each hour were summed up and statistica was performed for total counts from each 3 days for each group of mice.

## Statistical analysis

Statistical analyses were performed with two-tailed Student´s t-test for samples with homogenous variances with CI=95%. For samples with non-homogenous variances, non-parameteric Mann-Whitney's U test was applied. For more than one analyzed group, One-Way Analysis of Variance (ANOVA) with Duncan´s post-hoc test was used. All statistical calculations and graphs were made by using GraphPad Prism 7 software (GraphPad Software Inc., CA, USA). Levels for significances were as following: * $P<0.05$, ** $P<0.01$, *** $P<0.001$.

## AUTHOR DISCLOSURE STATEMENT

The authors declare no conflict of interests.


## ACKNOWLEDGEMENTS

We would like to thank the Turku Center for Disease Modeling (TCDM) personnel, specifically Nina Messner, Heli Niittymäki, Katri Hovirinta and Heidi Liljenbäck. Furthermore, we thank Taina Kirjonen, Anna Kostiander and Katariina Tanner for skillful technical assistance with the experiments and Biocenter Finland Cell Imaging Core (CIC) for using the laser capture microscope device.


## REFERENCES


1. Mendoza A, Hollenberg AN. New insights into thyroid hormone action. Vol. 173, Pharmacology and Therapeutics. 2017. p. 135–45.

2. Männistö T, Mendola P, Reddy U LS. Neonatal outcomes and birth weight in pregnancies complicated by maternal thyroid disease. Am J Epidemiol. 2013;178(5):731–40.

3. Kero J, Ahmed K, Wettschureck N, Tunaru S, Wintermantel T, Greiner E, et al. Thyrocyte-specific Gq/G11 deficiency impairs thyroid function and prevents goiter development. J Clin Invest. 2007;117(9):2399–407.

4. Grasberger H, Van Sande J, Mahameed AHD, Tenenbaum-Rakover Y, Refetoff S. Brief report: A familial thyrotropin (TSH) receptor mutation provides in vivo evidence that the inositol phosphates/Ca2+cascade mediates TSH action on thyroid hormone synthesis. J Clin Endocrinol Metab. 2007;92(7):2816–20.

5. Narumi S, Nagasaki K, Ishii T, Muroya K, Asakura Y, Adachi M, et al. Nonclassic TSH resistance: TSHR mutation carriers with discrepantly high thyroidal iodine uptake. J Clin Endocrinol Metab. 2011;96(8):E1340–5.

6. Vassart G, Dumont J. The thyrotropin receptor and the regulation of thyrocyte function and growth. Endocr Rev. 1992;13(3):596–611.

7. Kimura T, Van Keymeulen A, Golstein J, Fusco A, Dumont JE, Roger PP. Regulation of thyroid cell proliferation by TSH and other factors: a critical evaluation of in vitro models. Endocr Rev. 2001;22(5):631–56.

8. Germain-Lee EL, Schwindinger W, Crane JL, Zewdu R, Zweifel LS, Wand G, et al. A mouse model of albright hereditary osteodystrophy generated by targeted disruption of exon 1 of the Gnas gene. Endocrinology. 2005;146(11):4697–709.

9. Weinstein LS, Yu S, Warner DR, Liu J. Endocrine manifestations of stimulatory G protein α subunit mutations and the role of genomic imprinting. Vol. 22, Endocrine Reviews. 2001. p. 675–705.

10. Franco AT, Malaguarnera R, Refetoff S, Liao X-H, Lundsmith E, Kimura S, et al. Thyrotrophin receptor signaling dependence of Braf-induced thyroid tumor initiation in mice. Proc Natl Acad Sci. 2011;108(4):1615–20.

11. Lu C, Zhao L, Ying H, Willingham MC, Cheng SY. Growth activation alone is not sufficient to cause metastatic thyroid cancer in a mouse model of follicular thyroid carcinoma. Endocrinology. 2010;151(4):1929–39.

12. Michiels FM, Caillou B, Talbot M, Dessarps-Freichey F, Maunoury MT, Schlumberger M, et al. Oncogenic potential of guanine nucleotide stimulatory factor alpha subunit in thyroid glands of transgenic mice. Proc Natl Acad Sci U S A. 1994;91(22):10488–92.

13. Ledent C, Dumont JE, Vassart G, Parmentier M. Thyroid expression of an A2 adenosine receptor transgene induces thyroid hyperplasia and hyperthyroidism. EMBO J. 1992;11(2):537–42.

14. Guzo HI, Bircan R, Krohn K, Müller S, Vural S, Gezen C, et al. Similar prevalence of somatic TSH receptor and Gsα mutations in toxic thyroid nodules in geographical regions with different iodine supply in Turkey. Eur J Endocrinol. 2006;155(4):535–45.

15. Trülzsch B, Krohn K, Wonerow P, Chey S, Holzapfel H-PP, Ackermann F, et al. Detection of thyroid-stimulating hormone receptor and Gsα mutations: In 75 toxic thyroid nodules by denaturing gradient gel electrophoresis. J Mol Med. 2001;78(12):684–91.

16. Palos-Paz F, Perez-Guerra O, Cameselle-Teijeiro J, Rueda-Chimeno C, Barreiro-Morandeira F, Lado-Abeal J, et al. Prevalence of mutations in TSHR, GNAS, PRKAR1A and RAS genes in a large series of toxic thyroid adenomas from Galicia, an iodine-deficient area in NW Spain. Eur J Endocrinol. 2008 Nov;159(5):623–31.

17. J Parma L, Duprez J, Van Sande P, Cochaux C, Gervy J, Mockel J, Dumont G., Vassart, Schlechte JM. Somatic Mutations in the Thyrotropin Receptor Gene Cause Hyperfunctioning Thyroid Adenomas. Endocrinologist. 1994;4(2):152.

18. Kimura ET, Nikiforova MN, Zhu Z, Knauf JA, Nikiforov YE, Fagin JA. Advances in Brief High Prevalence of BRAF Mutations in Thyroid Cancer : Genetic Evidence for Constitutive Activation of the RET / PTC-RAS-BRAF Signaling Pathway in Papillary Thyroid Carcinoma. Cancer Res. 2003;63:1454–7.

19. Calebiro D, Grassi ES, Eszlinger M, Ronchi CL, Godbole A, Bathon K, et al. Recurrent EZH1 mutations are a second hit in autonomous thyroid adenomas. J Clin Invest. 2016;126(9):3383–8.

20. Boelaert K, Horacek J, Holder RL, Watkinson JC, Sheppard MC, Franklyn JA. Serum thyrotropin concentration as a novel predictor of malignancy in thyroid nodules investigated by fine-needle aspiration. J Clin Endocrinol Metab. 2006;91(11):4295–301.

21. Haugen BR, Alexander EK, Bible KC, Doherty GM, Mandel SJ, Nikiforov YE, et al. 2015 American Thyroid Association Management Guidelines for Adult Patients with Thyroid Nodules and Differentiated Thyroid Cancer: The American

Thyroid Association Guidelines Task Force on Thyroid Nodules and Differentiated Thyroid Cancer. Thyroid. 2016;26(1):1–133.

22. Stein SA, Oates EL, Hall CR, Grumbles RM, Fernandez LM, Taylor NA, et al. Identification of a point mutation in the thyrotropin receptor of the hyt/hyt hypothyroid mouse. Mol Endocrinol. 1994;8(2):129–38.

23. Marians RC, Ng L, Blair HC, Unger P, Graves PN, Davies TF. Defining thyrotropin-dependent and -independent steps of thyroid hormone synthesis by using thyrotropin receptor-null mice. Proc Natl Acad Sci U S A. 2002;99(24):15776–81.

24. Bianco AC, Anderson G, Forrest D, Galton VA, Gereben B, Kim BW, et al. American Thyroid Association Guide to investigating thyroid hormone economy and action in rodent and cell models. Thyroid. 2014;24(1):88–168.

25. Undeutsch H, Löf C, Offermanns S, Kero J. A mouse model with tamoxifen-inducible thyrocyte-specific cre recombinase activity. Genesis. 2014;52(4):333–40.

26. Chen M, Gavrilova O, Liu J, Xie T, Deng C, Nguyen AT, et al. Alternative Gnas gene products have opposite effects on glucose and lipid metabolism. Proc Natl Acad Sci U S A. 2005;102(20):7386–91.

27. Lyons J, Landis CA, Harsh G, Vallar L, Grunewald K, Feichtinger H, et al. Two G protein oncogenes in human endocrine tumors. Science. 1990;249(4969):655–9.

28. Xing M. Molecular pathogenesis and mechanisms of thyroid cancer. Vol. 13, Nature Reviews Cancer. NIH Public Access; 2013. p. 184–99.

29. Kim CS, Zhu X. Lessons from mouse models of thyroid cancer. Thyroid. 2009;19(12):1317–31.

30. Eszlinger M, Niedziela M, Typlt E, Jaeschke H, Huth S, Schaarschmidt J, et al. Somatic mutations in 33 benign and malignant hot thyroid nodules in children and adolescents. Mol Cell Endocrinol. 2014;393(1-2):39–45.

31. Pazaitou-Panayiotou K, Michalakis K, Paschke R. Thyroid cancer in patients with hyperthyroidism. Horm Metab Res = Horm und Stoffwechselforsch = Horm métabolisme. 2012;44(4):255–62.

32. Jaeschke H, Schaarschmidt J, Eszlinger M, Huth S, Puttinger R, Rittinger O, et al. A newly discovered TSHR variant (L665F) associated with nonautoimmune hyperthyroidism in an Austrian family induces constitutive TSHR activation by steric repulsion between TM1 and TM7. J Clin Endocrinol Metab. 2014;99(10):E2051–9.

33. Grasso P, Hinton RH. Evidence for and possible mechanisms of non-genotoxic carcinogenesis in rodent liver. Mutat Res - Fundam Mol Mech Mutagen. 1991;248(2):271–90.

34. Fiore E, Vitti P. Serum TSH and risk of papillary thyroid cancer in nodular thyroid disease. Vol. 97, Journal of Clinical Endocrinology and Metabolism. 2012. p. 1134–45.

35. Fiore E, Rago T, Provenzale MA, Scutari M, Ugolini C, Basolo F, et al. L-thyroxine-treated patients with nodular goiter have lower serum TSH and lower frequency of papillary thyroid cancer: Results of a cross-sectional study on 27 914 patients. Endocr Relat Cancer. 2010;17(1):231–9.

36. Franco AT, Malaguarnera R, Refetoff S, Liao X-H, Lundsmith E, Kimura S, et al. Thyrotrophin receptor signaling dependence of Braf-induced thyroid tumor initiation in mice. Proc Natl Acad Sci. 2011;108(4):1615–20.

37. Ariga M, Nedachi T, Akahori M, Sakamoto H, Ito Y, Hakuno F, et al. Signalling pathways of insulin-like growth factor-I that are augmented by cAMP in FRTL-5 cells. Biochem J. 2000;348(2):409.

38. Brewer C, Yeager N, Di Cristofano A. Thyroid-stimulating hormone-initiated proliferative signals converge in vivo on the mTOR kinase without activating AKT. Cancer Res. 2007;67(17):8002–6.

39. Zou M, Baitei EY, Al-Rijjal RA, Parhar RS, Al-Mohanna FA, Kimura S, et al. TSH overcomes Braf V600E-induced senescence to promote tumor progression via downregulation of p53 expression in papillary thyroid cancer. Oncogene. 2016;35(15):1909–18.

40. Orim F, Bychkov A, Shimamura M, Nakashima M, Ito M, Matsuse M, et al. Thyrotropin Signaling Confers More Aggressive Features with Higher Genomic Instability on BRAF V600E -Induced Thyroid Tumors in a Mouse Model. Thyroid. 2014;24(3):502–10.

41. Rakov H, Engels K, Hönes GS, Brix K, Köhrle J, Moeller LC, et al. Sex-specific phenotypes of hyperthyroidism and hypothyroidism in aged mice. Biol Sex Differ. 2017;8(1):36.

42. Riese C, Michaelis M, Mentrup B, Götz F, Köhrle J, Schweizer U, et al. Selenium-dependent pre- and posttranscriptional mechanisms are responsible for sexual dimorphic expression of selenoproteins in murine tissues. Endocrinology. 2006;147(12):5883–92.

43. Hervas F, De Escobar GM, Del Rey FE. Rapid effects of single small doses of L-thyroxine and triiodo-L-thyronine on growth hormone, as studied in the rat by radioimmunoassay. Endocrinology. 1975;97(1):91–101.

44. Jeker LT, Hejazi M, Burek CL, Rose NR, Caturegli P. Mouse thyroid primary culture. Biochem Biophys Res Commun. 1999;257(2):511–5.

45. Harper JF, Brooker G. Femtomole sensitive radioimmunoassay for cyclic AMP and cyclic GMP after 2'0 acetylation by acetic anhydride in aqueous solution. J Cycl Nucleotide Res. 1975;1(4):207–18.

46. Undeutsch H, Löf C, Pakarinen P, Poutanen M, Kero J. Thyrocyte-specific Dicer1 deficiency alters thyroid follicular organization and prevents goiter development. Endocrinology. 2015;156(4):1590–601.

## FIGURES

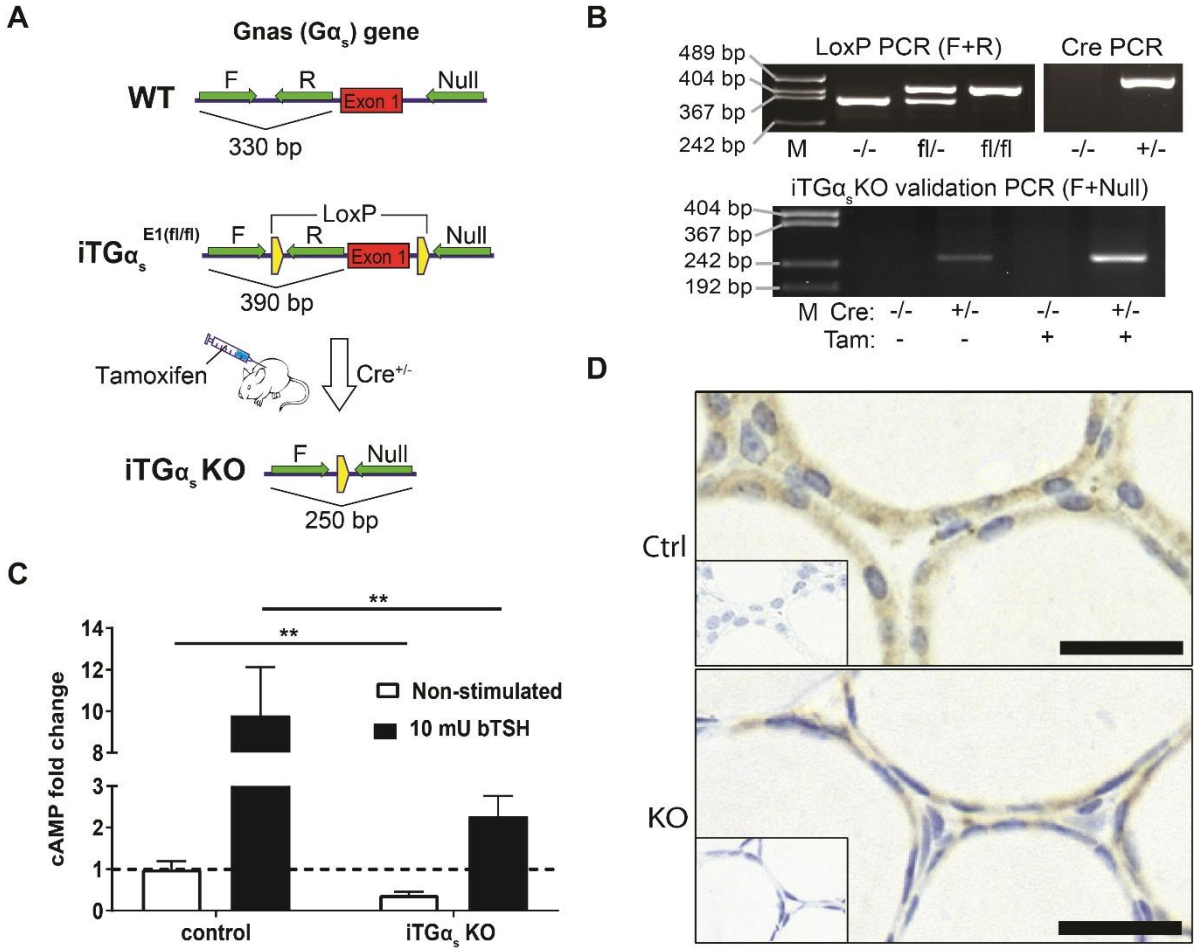


**Figure 1: Generation and validation of the tamoxifen-inducible thyrocyte-specific Gα$_s$-deficient (iTGα$_s$KO) mice.** A) Outline of the generation strategy of the iTGα$_s$KO mouse line. (F = (forward), R = (reverse) and Null - genotyping primers, WT – wild type (330 bp); iTGα$_s$E1 (fl/fl) – Gα$_s$ Exon 1 floxed (fl/fl) homozygous (390 bp); Cre$^{+/-}$ – Cre recombinase expressing heterozygous mouse under thyroglobulin (Tg) promoter; iTGα$_s$KO – thyrocyte-specific tamoxifen-inducible homozygously Gα$_s$-deficient mouse (250 bp). B) Analysis of the recombination by PCR using genomic DNA. fl/fl – LoxP floxed homozygous; fl/- – LoxP floxed heterozygous; -/- – wild type; +/- – Cre recombinase heterozygous; Tam- – vehicle treated; Tam+ – tamoxifen treated mouse. C) cAMP measurements of the basal and TSH-stimulated primary thyrocytes of the control and iTGα$_s$KO mice. ** = P<0.01. D) Immunohistochemical analysis of the control (Ctrl) and iTGα$_s$KO (KO) thyroids using anti-Gα$_s$ antibody. Small picture: negative control without primary antibody; Scale bar: 25 μm.

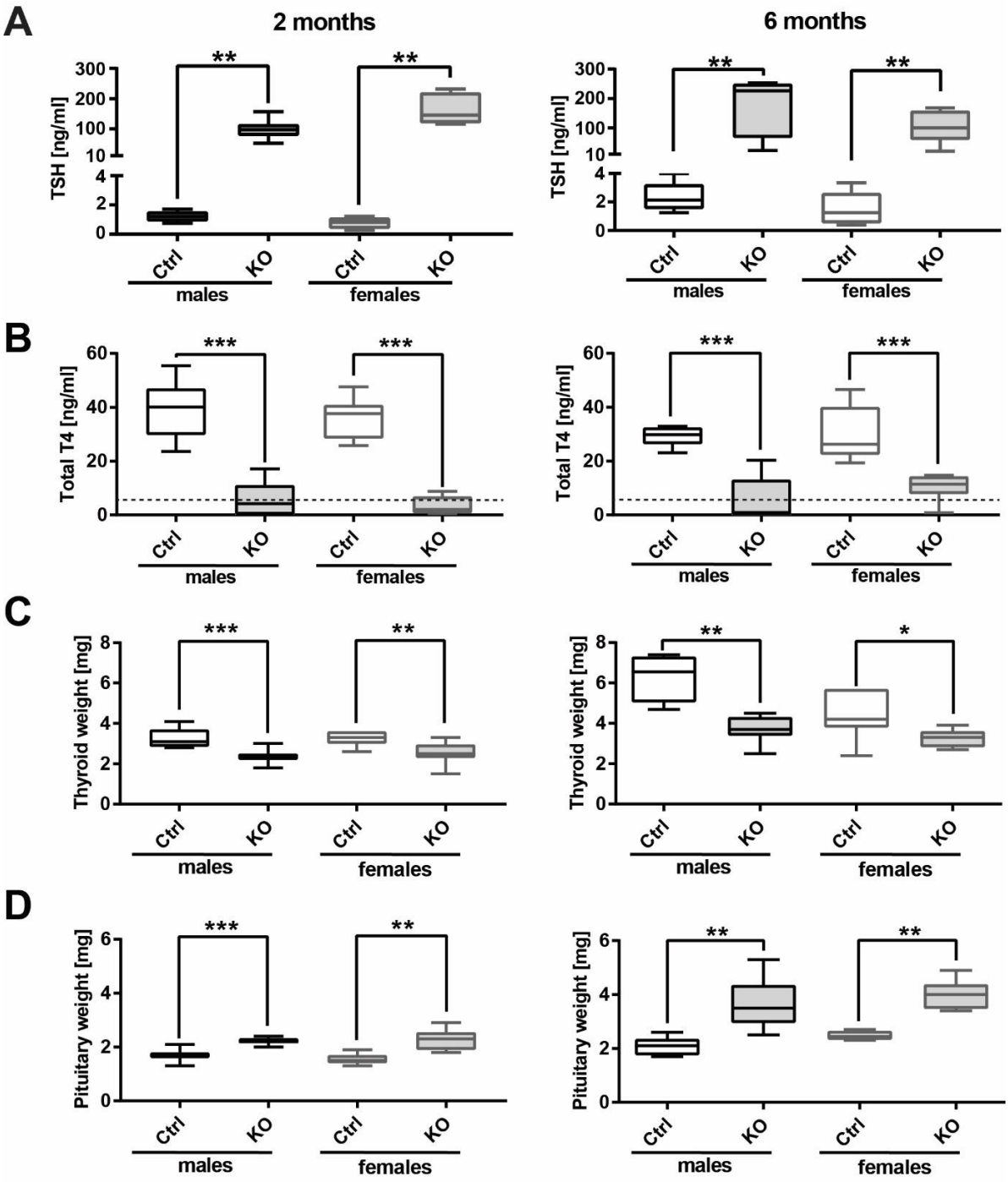


**Figure 2**: **Thyroid function test, thyroid and pituitary weights in the iTG$\alpha_s$KO and control animals.** A) serum TSH, B) total T4 concentrations, C) thyroid and D) pituitary weights in 2 and 6 months old control and iTG$\alpha_s$KO mice. Ctrl – control mice ($Cre^{-/-}$, $G\alpha_s^{fl/fl}$, Tam); KO - iTG$\alpha_s$KO mice ($Cre^{+/-}$, $G\alpha_s^{fl/fl}$, Tam); Dotted line – assay detection limit; Whiskers show minimum and maximum value, lower box line: 25$^{th}$ percentile; middle box line: median; upper box line: 75$^{th}$ percentile; * = P <0.05; ** = P<0.01; *** = P<0.001.

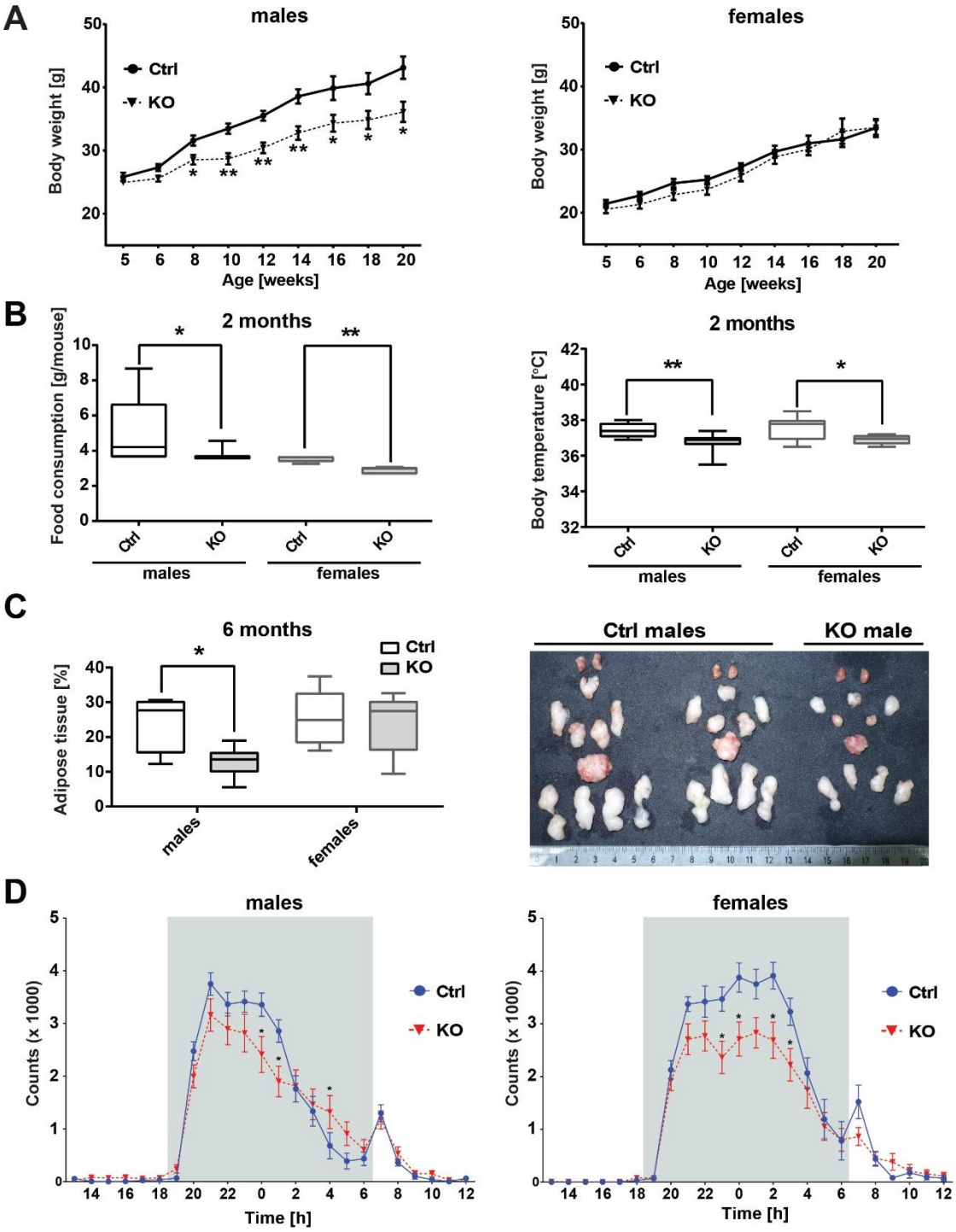


**Figure 3: Metabolic consequences of the hypothyroidism in the iTGα$_s$KO mice**. A) Body weight of the iTGα$_s$KO mice and controls at age of 5-20 weeks (n = 9/group). Ctrl – control mice (Cre$^{-/-}$ Tam); KO - iTGα$_s$KO mice (Cre$^{+/-}$ Tam). B) Food consumption (left) and body temperature (right) of the 2 months old iTGα$_s$KO mice and controls. C) EchoMRI measurement of mass percentage (left) and picture of total adipose tissue (right) of 6 month old iTGα$_s$KO mice. D) Activity of 2 months old iTGα$_s$KO mice and controls. Grey background – night cycle. Ctrl – control mice (Cre$^{-/-}$, Gα$_s^{fl/fl}$, Tam); KO - iTGα$_s$KO mice (Cre$^{+/-}$, Gα$_s^{fl/fl}$, Tam); Whiskers show minimum and maximum value, lower box line: 25$^{th}$ percentile; middle box line: median; upper box line: 75$^{th}$ percentile; * = P <0.05; ** = P<0.01.

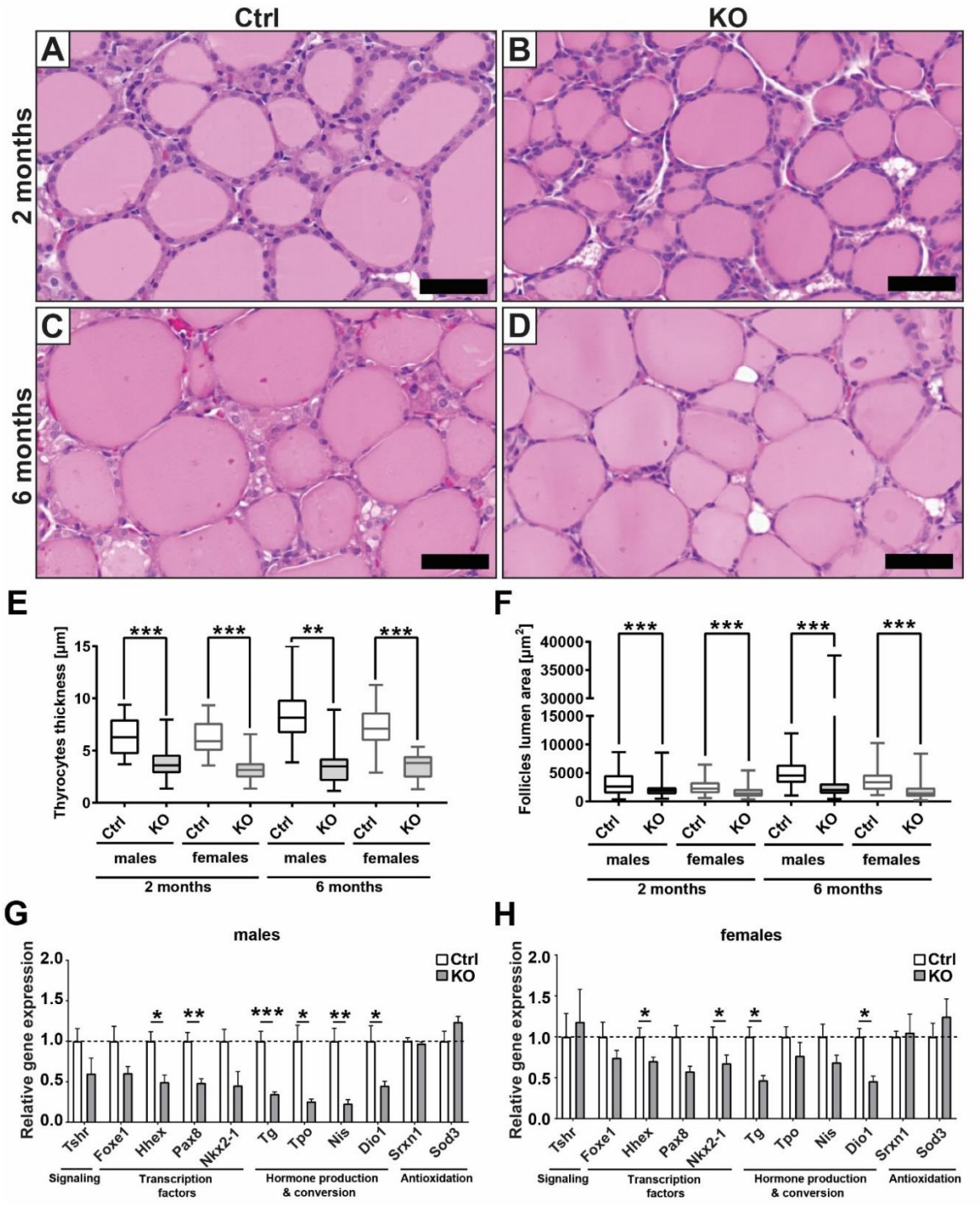


**Figure 4: Thyroid histology, morphometric analysis and gene expression in the iTG$\alpha_s$KO mice.** Histology (HE) of the control (A, C) and iTG$\alpha_s$KO (B, D) thyroids from 2- and 6-month-old animals, respectively. scale bar: 50 µm. Morphometric analysis of thyrocyte thickness (E) and follicles area (F) of controls and the iTG$\alpha_s$KO thyroids. Whiskers show minimum and maximum value, lower box line: 25$^{th}$ percentile; middle box line: median; upper box line: 75$^{th}$ percentile. Gene expression analysis of thyroid specific genes and genes involved in antioxidation in 6 months old iTG$\alpha_s$KO male (G) and female (H) thyroids. Ctrl – control mice (Cre$^{-/-}$, G$\alpha_s^{fl/fl}$, Tam); KO - iTG$\alpha_s$KO mice (Cre$^{+/-}$, G$\alpha_s^{fl/fl}$, Tam); Error bars show SEM value; * = P <0.05; ** = P<0.01; *** = P<0.001.

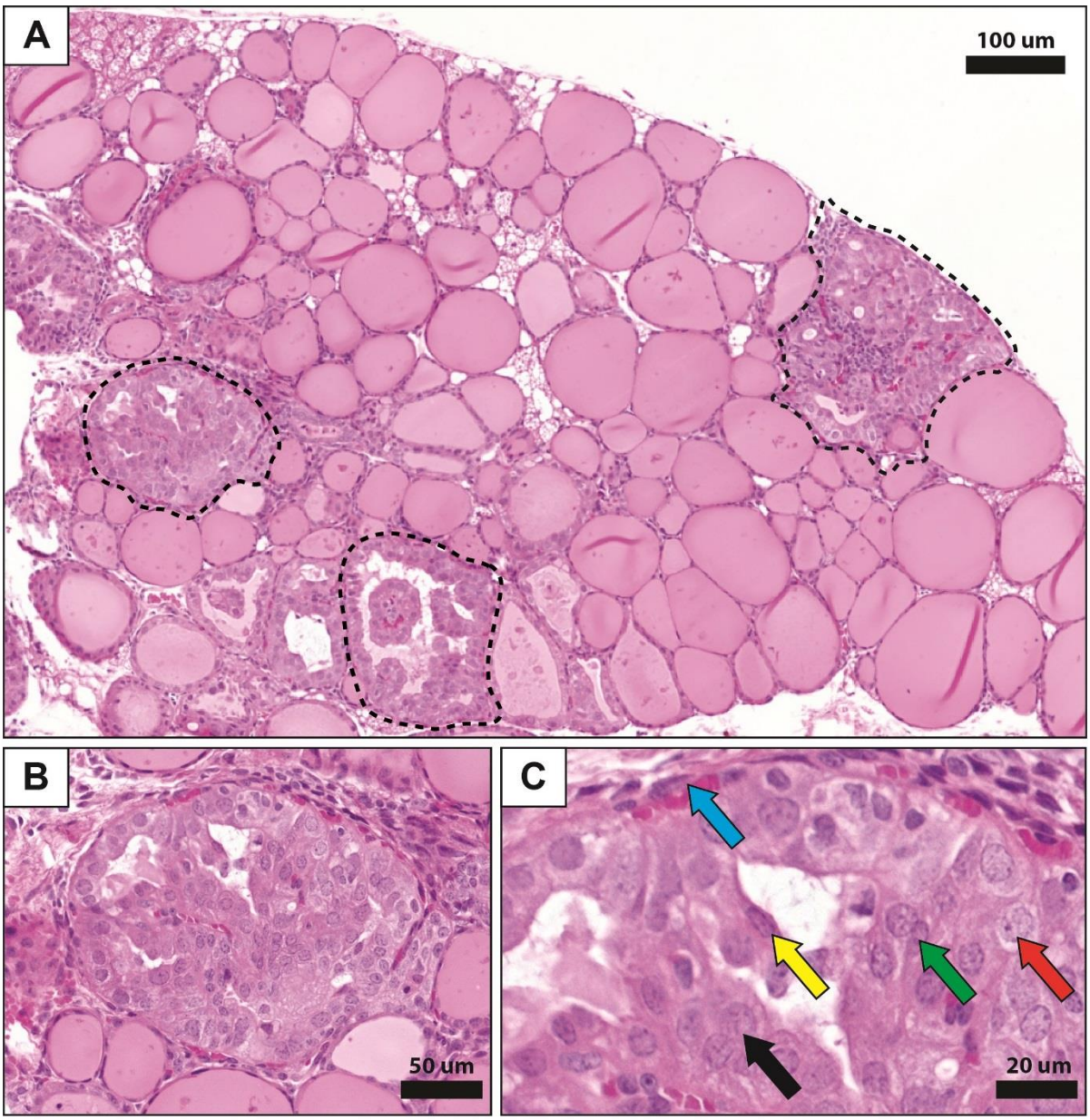


**Figure 5: Hyperplastic and papillary thyroid carcinoma-like (PTC-like) lesions in the 6 months old iTG$\alpha_s$KO mice.** A) HE staining of male iTG$\alpha_s$KO mouse thyroid, PTCs-like areas marked with dotted line B) and C) higher magnifications of the PTC-like lesions with the typical PTC features marked with symbols: capsule (blue arrow), elongated nuclei (yellow arrow), overlapping nuclei (green arrow), enlarged nuclei (red arrow) and grooves (black arrow).

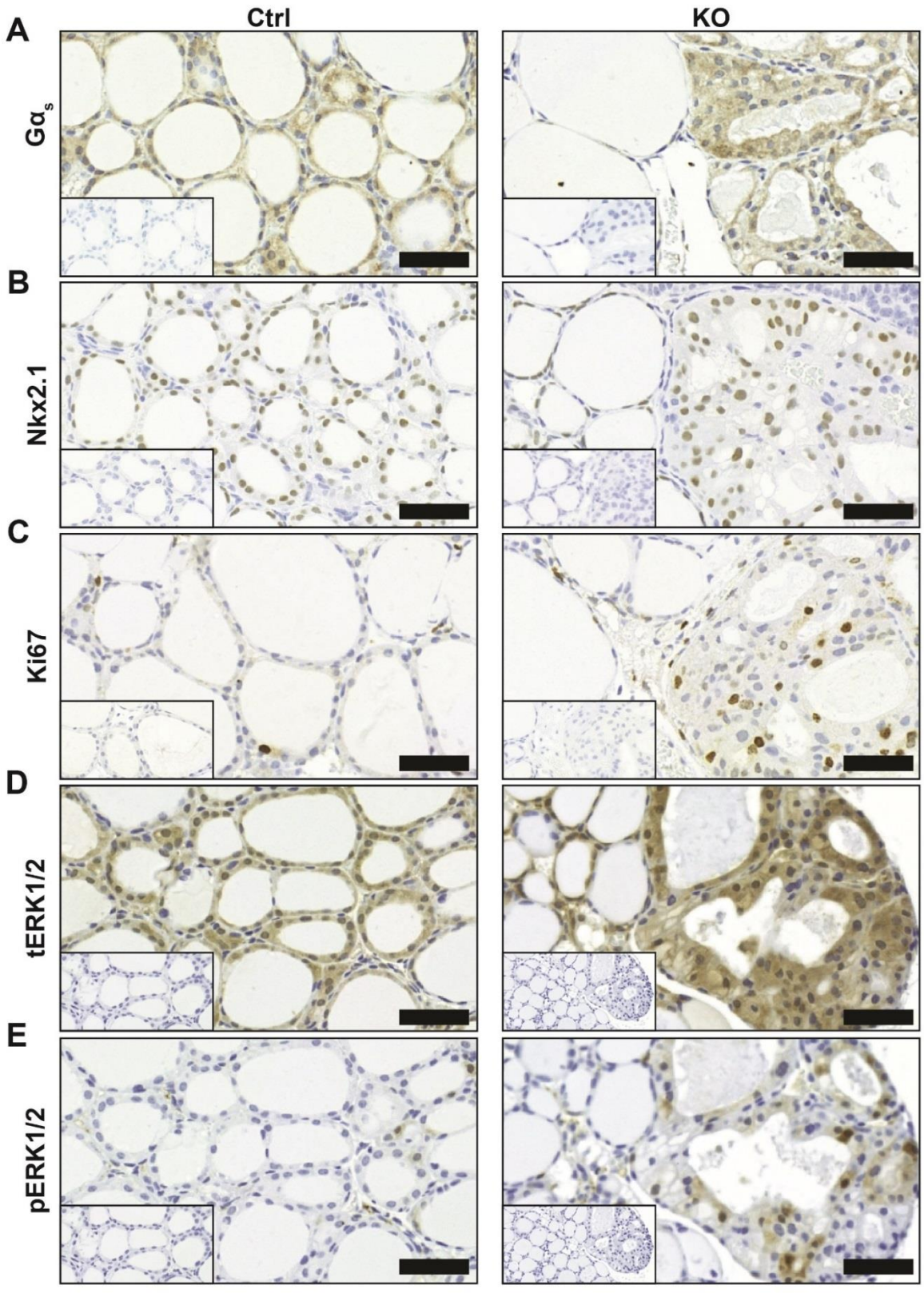


**Figure 6: IHC analysis of 6 months old iTGαsKO thyroids with PTC-like areas.** IHC stainings with antibodies against A) $G\alpha_s$, B) Nkx2.1, C) Ki67, D) total-Erk1/2, E) phospho-Erk1/2. Antibodies used for the staining's are listed in the Table 2. Ctrl – control mice ($Cre^{-/-}$, $G\alpha_s^{fl/fl}$, Tam); KO - iTG$\alpha_s$KO mice ($Cre^{+/-}$, $G\alpha_s^{fl/fl}$, Tam); Scale bar: 50 µm.

## SUPPLEMENTARY FIGURES AND TABLES

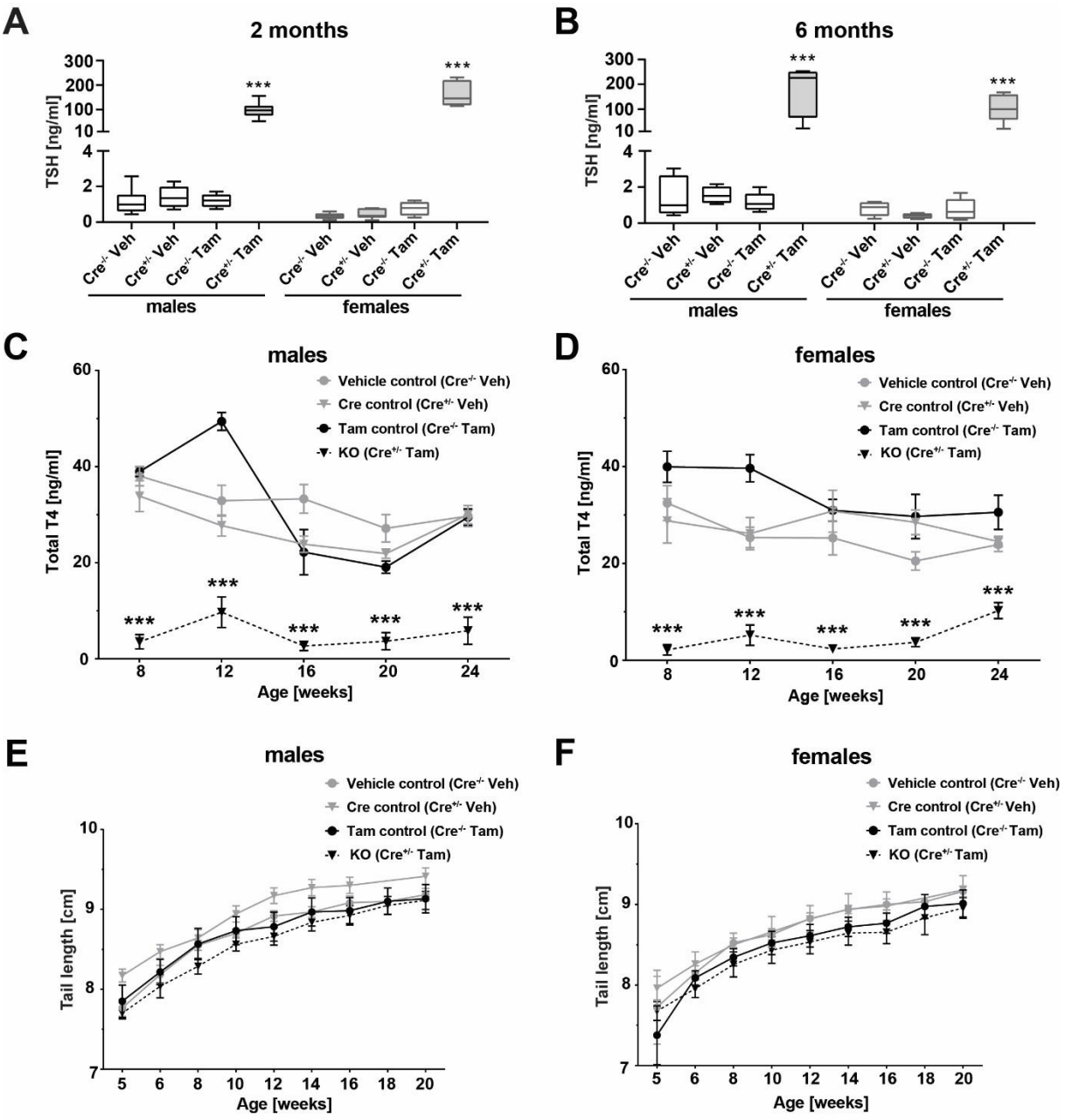


**Supplementary figure 1: Characterization of all control groups.** TSH concentration in A) 2 months and B) 6 months old control mice. Total T4 concentration in 8 - 24 weeks old control and iTG$\alpha_s$KO C) males and D) females. Tail length in 5 - 20 weeks old control and iTG$\alpha_s$KO E) males and F) females. $Cre^{+/-}$ – Cre recombinase expressing mouse; $Cre^{-/-}$ – Cre recombinase non-expressing mouse; Tam – tamoxifen treated mouse; Veh – vehicle treated mouse; KO - iTG$\alpha_s$KO mice; iTG$\alpha_s$KO group was compared with Tam control group; Error bars show SEM value; * = P <0.05; ** = P<0.01; *** = P<0.001.

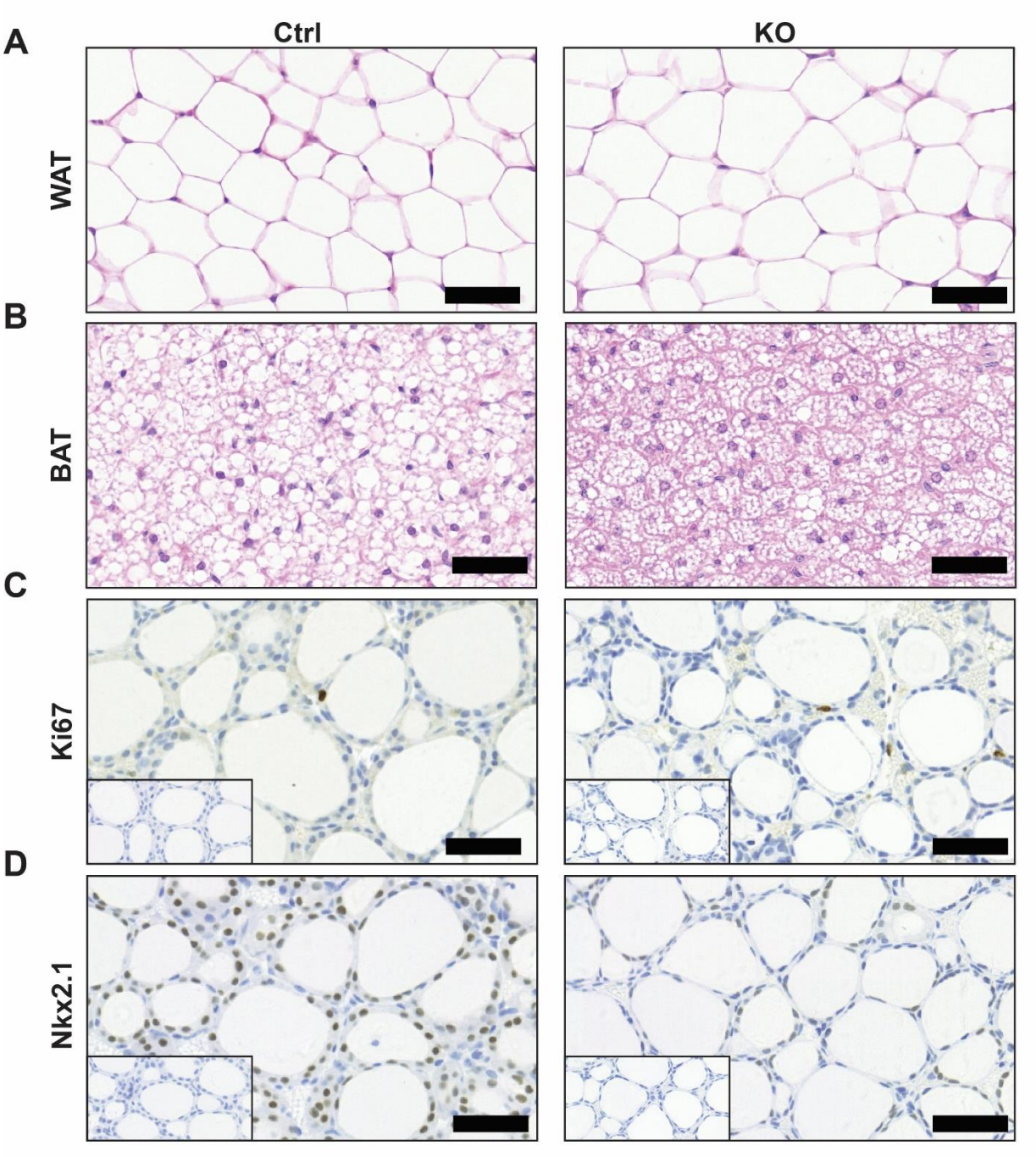


**Supplementary figure 2: Adipose tissue characterization and thyroid proliferation analysis in the iTGα$_s$KO mice.** White (WAT) A) and Brown (BAT) B) adipose tissue in the 6 months old iTGα$_s$KO mice. C) Ki67 and D) Nkx2.1 staining in the thyroid of 2 months old iTGα$_s$KO mice. Ctrl – control mice (Cre$^{-/-}$, Gα$_s^{fl/fl}$, Tam); KO - iTGα$_s$KO mice (Cre$^{+/-}$, Gα$_s^{fl/fl}$, Tam); Scale bar: 50 µm.

## Table 1: List of qRT-PCR primers

| Gene | Forward primer | Reverse primer |
|---|---|---|
| ***Tshr*** | 5'- CCATCTCCTTCTATGCGCTGTCG - 3 | 5'- GCTGAGCAGGATGAACACGTCC - 3 |
| ***Foxe1*** | 5'- GACTCTGGGCGGCATCTACAAGTT - 3 | 5'- TTGAGGAAGCAGTCGTTGAGGGT - 3 |
| ***Hhex*** | 5'- CGGACGGTGAACGACTACAC - 3 | 5'- CGTTGGAGAACCTCACTTGAC - 3 |
| ***Pax8*** | 5'- CCTGCTGAGTTCTCCATATTATTAC - 3 | 5'- CCTTTGTGTGACTCTCTGGG - 3' |
| ***Nkx2.1*** | 5'- CAGCCGACGCCGAATCAT - 3' | 5'- CTGGCCCTGTCTGTACGC - 3' |
| ***Tg*** | 5'- CTTATGGGAGGCTCTGCAC - 3' | 5'- CACAGCCAGGAGCTTGGTC -3' |
| ***Tpo*** | 5'- CAAAGGCTGGAACCCTAATTTCT - 3' | 5'- AACTTGAATGAGGTGCCTTGTCA - 3' |
| ***Nis*** | 5'- GGGATGCACCAATGCCTCTG - 3' | 5'- GTAGCTGATGAGAGCACCACA - 3' |
| ***Dio1*** | 5'- GGGCAGGATCTGCTACAAGG - 3 | 5'- CGTGTCTAGGTGGAGTGCAA - 3 |
| ***Srxn1*** | 5'- CCCAGGGTGGCGACTACTA - 3 | 5'- GTGGACCTCACGAGCTTGG - 3 |
| ***Sod3*** | 5'- CCTTCTTGTTCTACGGCTTGC - 3 | 5'- TCGCCTATCTTCTCAACCAGG - 3 |
| ***Ppia*** | 5'- CATCCTAAAGCATACAGGTCCTG - 3' | 5'- TCCATGGCTTCCACAATGTT - 3' |
| ***Rpl19*** | 5'- CTGAAGGTCAAAGGGAATGTG - 3' | 5'- GGACAGAGTCTTGATGATCTC - 3' |

## Table 2: List of antibodies

| Antigen | Isotype / Clonality (clone) | Manufacture (Cat. No.) | Dilution | Application |
|---|---|---|---|---|
| **$G\alpha_s$** | Rabbit IgG / polyclonal (-) | Abcam (83735) | 1:150 | IHC |
| **KI67** | Rat IgG2a / monoclonal (SolA15) | eBioscience (14-5698-80) | 1:2000 | IHC |
| **NKX2.1** | Mouse / monoclonal (8G7G3/1) | Dako (M3575) | 1:200 | IHC |
| **ERK1/2** | Rabbit IgG / monoclonal (137F5) | Cell signaling Technology, Inc (4695) | 1:250 | IHC |
| **Phospho-ERK1/2** | Rabbit IgG/ monoclonal (D13.14.4E) | Cell signaling Technology, Inc (4370) | 1:400 | IHC |